Research Square

Preprints are preliminary reports that have not undergone peer review.
They should not be considered conclusive, used to inform clinical practice,
or referenced by the media as validated information.

Multi Objective Sensor Network Layout Optimization Method Based on Reference Point Sorting Mechanism

Qin Wang

QinWang291@163.com

Suzhou Vocational Institute of Industrial Technology

Lihua Dai

Suzhou Vocational Institute of Industrial Technology

Research Article

Keywords: Wireless sensor network, Multi objective optimization, Sorting of reference points, Layout optimization, energy balance

Posted Date: May 14th, 2026

DOI: https://doi.org/10.21203/rs.3.rs-9242434/v1

License: This work is licensed under a Creative Commons Attribution 4.0 International License.
Read Full License

Additional Declarations: No competing interests reported.

Multi Objective Sensor Network Layout Optimization Method Based on Reference Point Sorting Mechanism

Qin Wang*, Lihua Dai

School of Electronic and Communication Engineering, Suzhou Vocational Institute of Industrial Technology, SuZhou, JiangSu 215104, China

*corresponding author:Qin Wang

Qin Wang's e-mail:QinWang291@163.com

Lihua Dai's e-mail:LiHuaDai9@126.com

Abstract: This paper proposes a multi-objective optimization method based on reference point sorting mechanism (R-MOTS) for the layout optimization problem of wireless sensor networks (WSN), aiming to solve the limitations of traditional non dominated sorting algorithms in terms of uneven distribution of solution sets, missing edge solutions, and insufficient convergence accuracy. By embedding the reference point sorting mechanism into the multi-objective Transit Search (MOTS) framework, combined with individual density estimation and columnar grid filtering mechanism, the diversity maintenance ability and search efficiency of the algorithm have been significantly improved. The experimental results show that R-MOTS achieves an average improvement of 16.3% in IGD metrics and 12.7% in solution set uniformity on standard test functions such as ZDT, DTLZ, and UF series. It also achieves 92.67% coverage and 1078 rounds of network lifetime in complex WSN deployment scenarios, outperforming traditional algorithms such as NSGA-II and MOPSO.

Keywords: Wireless sensor network; Multi objective optimization; Sorting of reference points; Layout optimization; energy balance

1 Introduction

Wireless sensor networks (WSN), as the core supporting technology of the Internet of Things, play an irreplaceable role in fields such as environmental monitoring, smart cities, and industrial control [1-2]. With the continuous expansion of the global WSN market, its deployment complexity has significantly increased, and node layout optimization has become a fundamental issue to ensure network perception capability, energy balance, and lifecycle.

Traditional single objective optimization methods are difficult to coordinate conflicts between multiple objectives such as coverage, energy balance, and connectivity, and there is an urgent need for efficient multi-objective optimization algorithms to achieve optimal global resource allocation [3]. The current research focus has shifted towards balancing the competitive relationships between multidimensional targets through intelligent algorithms to address the challenges posed by complex terrain, dynamic obstacles, and heterogeneous nodes. However, the shortcomings of algorithms in solution set distribution, computational efficiency, and environmental adaptability remain the core bottlenecks that constrain practical deployment.

In recent years, multi-objective evolutionary algorithms have made significant progress in WSN layout optimization. Harizan et al. proposed a relay node deployment strategy based on multi-objective evolutionary algorithm, which reduces energy consumption and improves connectivity by optimizing inter cluster communication paths, confirming the effectiveness of the decomposition strategy in balancing network lifetime and coverage redundancy [4]. Prakash and Kalaivani further integrated swarm intelligence ideas and designed a hybrid firefly cat swarm algorithm to solve node localization problems. Its adaptive mechanism showed better convergence than traditional genetic algorithms in heterogeneous networks [5]. Zhou et al. constructed a multi constraint optimization model for visual sensor networks in target tracking scenarios, and introduced a spatial position encoding strategy to significantly improve target capture accuracy, highlighting the importance of problem specific modeling [6]. Poongavanam et al. used multi-objective frog leaping algorithm to optimize the deployment of goal oriented WSN, and dynamically adjusted the population distribution to reduce redundant nodes, verifying the potential of heuristic algorithms in reducing hardware costs [7]. These studies have jointly promoted the application depth of multi-objective optimization theory in the field of WSN, but there are still significant limitations in the algorithm's adaptability to dynamic environments and the uniformity of the distribution of solution sets in high-dimensional objective spaces.

Although existing methods have achieved certain results, their inherent limitations have constrained the deployment efficiency in complex scenarios. Firstly, traditional non dominated sorting algorithms such as NSGA-II are prone to uneven distribution of solution sets and missing edge solutions in high-dimensional objective spaces, making it difficult to

fully cover the sparse areas of the Pareto front and reducing the decision value of the scheme [8-9]. Secondly, decomposition based algorithms (such as MOEA/D) rely on static weight vectors, which are difficult to adapt to environmental changes caused by dynamic obstacles, and the computational complexity increases exponentially with the increase of the target dimension. In addition, swarm intelligence algorithms such as MOPSO have insufficient stability when dealing with nonlinear constraints, and are prone to getting stuck in local optima in deployments with occluded terrain, resulting in coverage fluctuations exceeding 15% [10-11]. It is particularly prominent that existing research generally lacks a collaborative optimization mechanism for energy balance and coverage redundancy, and the real-time response capability under node overlap perception and mobile obstacle interference is insufficient, which limits the further improvement of network lifecycle and robustness.

In response to the above challenges, this paper proposes a multi-objective sensor network layout optimization method based on reference point sorting mechanism (R-MOTS). By embedding the reference point guidance strategy into the multi-objective Transit Search framework, the non dominated sorting and diversity preservation mechanism is reconstructed: 1) Design a reference point vertical distance metric to replace traditional congestion calculation, enhancing the exploration ability of the Pareto frontier edge region; 2) Combining the adaptive filtering mechanism of columnar grid to dynamically partition the target space, and allocating grid capacity based on sparsity weights to balance the distribution of solution sets; 3) Introduce an energy weighted joint perception probability model and dynamic connectivity constraints to construct a coverage energy consumption connectivity collaborative optimization objective function. This scheme significantly improves the adaptability of the algorithm in dynamic obstacle environments, while controlling computational complexity through lightweight index structures [12-13]. Experimental verification shows that R-MOTS outperforms mainstream algorithms in solution set convergence, distribution uniformity, and actual deployment metrics, providing an efficient optimization paradigm for complex WSN scenarios.

2 Optimization modeling of wireless sensor networks

2.1 Node Coverage Model

The modeling of node perception range aims to accurately describe the perception capability and spatial distribution characteristics of sensor nodes. This author adopts the Probabilistic Sensing Model to more accurately characterize the spatial distribution of node perception capabilities. Let S={s1, s2,..., sn} represent the set of n sensor nodes in WSN, and the position coordinates of each node si are (xi, yi, zi) [14]. For any target point p (x, y, z) in the monitoring area, the perception probability of node si can be represented by the following function, as shown in equation (1):

$$P_{s_i}(p)=\begin{cases}1, & \text{if} d(s_i,p)\le d_1\\ e^{-\alpha(d(s_i,p)-d_1)^{\beta}}, & \text{if} d_1<d(s_i,p)\le d_2\\ 0, & \text{if} d(s_i,p)>d_2\end{cases} \quad (1)$$

Among them, d (si, p) represents the Euclidean distance between sensor node si and target point p, calculated by the following formula (2):

$$d(s_i,p)=\sqrt{(x_i-x)^2+(y_i-y)^2+(z_i-z)^2} \quad (2)$$

Parameters d1 and d2 respectively represent the determined sensing radius and maximum sensing radius of the sensor, satisfying 0<d1<d2. Parameters α and β are attenuation coefficients related to specific sensor types, determining the rate at which perceptual ability decays with distance [15]. In addition, environmental factors such as obstacles, noise, and interference can also affect the perception effect, which can be corrected by introducing the environmental attenuation coefficient λ_{env}, as shown in equation (3):

$$P_{s_i,env}(p)=P_{s_i}(p)\cdot\lambda_{env} \quad (3)$$

In order to quantify the coverage efficiency of the entire network, the area coverage index C_R is defined. Assuming that the monitoring area R can be discretized into m sampling points \ {p1, p2,..., pm}, the coverage can be expressed as the following equation (4):

$$C_R=\frac{1}{m}\sum_{j=1}^{m}\delta\left(p_j\right) \quad (4)$$

Where $\delta\left(p_j\right)$ is the judgment function, when the sampling point p_j is effectively perceived by at least one sensor node (i.e., when the perception probability exceeds the preset threshold Pth, $\delta\left(p_j\right)=1$, otherwise $\delta\left(p_j\right)=0$.

In actual deployment of wireless sensor networks, the monitoring area is usually covered by multiple sensor nodes, forming redundant perception and improving system reliability and robustness [16-17]. Therefore, building a probability model for multi node joint perception is

crucial for evaluating the overall performance of the network. For any target point p in the monitoring area, assuming that there are k sensor nodes $\{s_{i_1}, s_{i_2}, ..., s_{i_k}\}$ that can perceive the point, it is necessary to determine the joint perception probability of these nodes [18]. Based on the assumption of independent perception, the joint probability formula can be used to calculate the probability that the target point p is successfully perceived by at least one node, as shown in equation (5):

$$P_{joint}(p)=1-\prod_{j=1}^{k}\left(1-P_{s_{ij}}(p)\right) \tag{5}$$

Considering the computational complexity, an approximate calculation method can be introduced. When there are a large number of nodes, Monte Carlo simulation method can be used to evaluate the joint probability of multiple nodes, or Poisson distribution approximation can be used, as shown in equation (6):

$$P_{approx}(p) = 1 - e^{-\sum_{j=1}^{k} P_{s_{ij}}(p)} \tag{6}$$

This approximation works well when the number of nodes is large and the perception probability of a single node is low. In practical applications, collaborative perception between nodes also involves energy consumption optimization issues. In response to this demand, an energy weighted joint perception probability model can be proposed, as shown in equation (7):

$$P_{energy}(p) = \frac{\sum_{j=1}^{k} w_j \cdot P_{s_{ij}}(p)}{\sum_{j=1}^{k} w_j} \tag{7}$$

Among them, the weight coefficient w_j is proportional to the remaining energy of node s_{ij}, which can achieve network load balancing and extend the overall lifecycle. For different types of perception data, multi node fusion strategies also vary. These fusion strategies can be expressed as a universal probability fusion function F, as shown in equation (8):

$$P_{fusion}(p) = F\left(P_{s_{i_1}}(p), P_{s_{i_2}}(p), \ldots, P_{s_{i_k}}(p), \Theta\right) \tag{8}$$

Among them, Θ represents the fusion parameter set, customized according to specific application scenarios.

2.2 Calculation methods for single point coverage and global area coverage

In the layout optimization of wireless sensor networks (WSN), coverage is the core indicator for evaluating network perception capability. This section integrates the single point coverage model with the calculation method of global area coverage, providing a theoretical basis for multi-objective optimization [19-20].

The coverage capability of sensor nodes on target points is described using a probability model. Assuming the node position is s and the target point is p, the perception probability formula is as follows (9):

$$P_{cov}(s,p)=\begin{cases}1, & \text{if} d(s,p)\le R_s-R_e\\ e^{-\alpha\frac{(d(s,p)-(R_s-R_e))^{\beta}}{R_e}}, & \text{if} R_s-R_e<d(s,p)<R_s+R_e\\ 0, & \text{if} d(s,p)\ge R_s+R_e\end{cases} \tag{9}$$

Among them, $d(s,p)$ represents the Euclidean distance between node s and target point p, R_s represents the nominal sensing radius of the sensor, R_e represents the range of sensing uncertainty, and α and β are adjustment parameters that control the sensing attenuation rate and curve shape, respectively [21]. This model is more suitable for complex environments than binary coverage. When multiple nodes cover the same target point, the joint coverage probability is calculated based on the assumption of independence as shown in equation (10):

$$P_{joint}(p)=1-\prod_{i=1}^{n}\left(1-P_{cov}(s_i,p)\right) \tag{10}$$

If $P_{joint}(p)\ge\theta$ (threshold often set at 0.9 or 0.95), it is considered that point p is effectively covered. The global coverage is calculated using grid discretization method. Divide the area into a set of m × m grid points G, and the coverage formula is given by equation (11):

$$\text{Coverage}=\frac{1}{|G|}\sum_{p\in G}I\left(P_{joint}(p)\ge\theta\right) \tag{11}$$

An adaptive grid partitioning strategy can be used to balance accuracy and efficiency: fine-grained grids are used for dense areas, and coarse-grained grids are used for sparse areas.

In addition to coverage, coverage uniformity (Redundancy) and keypoint coverage (KeyCoverage) also need to be considered in multi-objective WSN optimization, as shown in equations (12) and (13):

$$\text{Redundancy}=\frac{1}{|G|}\sum_{p\in G}\left(\sum_{i=1}^{n} I(P_{cov}(s_i, p)\geq\theta)-1\right)^{+} \quad (12)$$

$$\text{KeyCoverage}=\frac{1}{|K|}\sum_{p\in K} I\left(P_{joint}(p)\geq\theta_k\right) \quad (13)$$

Among them, $(x)^{+}$represents max (x, 0), which reflects how many sensors effectively cover each grid point. Measure the variance of coverage probability through grid points. θ_k is usually higher than the coverage threshold of ordinary grid points to ensure high-quality perception of critical areas [22].

2.3 Energy consumption model

The energy consumption problem in wireless sensor networks (WSN) is a key factor affecting the network lifecycle, mainly derived from node movement, signal transmission, and perception radiation processes [23]. This section constructs a comprehensive energy consumption model and introduces a low coverage penalty strategy to balance the contradiction between energy consumption and coverage quality. The energy consumption of node mobility can be expressed as the following equation (14):

$$E_{move}(i)=\mu\times d_i \quad (14)$$

Among them, $E_{move}(i)$ represents the mobile energy consumption of node i, μ is the mobile energy consumption coefficient (related to factors such as node weight and terrain characteristics), and d_i represents the distance traveled by node i. For complex terrains, the energy consumption of movement also needs to consider the influence of slope, which can be extended to the following equation (15):

$$E_{move}(i)=\mu\times d_i\times\left(1+\theta\times\tan(\alpha_i)\right) \quad (15)$$

θ is the slope influence coefficient, and α_i is the average slope angle of node i's movement path. The energy consumption of signal transmission is based on classical wireless communication theory, as shown in equation (16):

$$E_{tx}(k, d)=E_{elec}\times k+\epsilon_{amp}\times k\times d^{n} \quad (16)$$

Here, $E_{tx}(k, d)$ represents the energy required to send k-bit data to a receiving node at a distance of d, E_{elec} is the circuit energy consumption coefficient, ϵ_{amp} is the amplifier energy consumption coefficient, and n is the path loss index (usually between 2-6, varying depending on the environment). Correspondingly, the energy consumption model for

receiving data is as follows (17):

$$E_{rx}(k)=E_{elec}\times k \tag{17}$$

$E_{rx}(k)$ represents the energy consumed to receive k-bit data. In the scenario of multi hop transmission, the relay node needs to receive and forward data, and its energy consumption is as follows (18):

$$E_{relay}(k,d)=E_{rx}(k)+E_{tx}(k,d)=2E_{elec}\times k+\epsilon_{amp}\times k\times d^{n} \tag{18}$$

The energy consumption of node radiation mainly comes from the perception process. Based on common radiation models, the energy consumption of a node performing a perception operation can be modeled as equation (19):

$$E_{sens}=\beta\times\pi\times R_s^2 \tag{19}$$

Among them, E_{sens} is the single perception energy consumption, β is the perception energy consumption coefficient, and Rs is the perception radius of the node. Based on the above energy consumption components, the total energy consumption model of a single node i can be expressed as the following equation (20):

$$E_{total}(i)=E_{move}(i)+\eta_1\times E_{tx}(i)+\eta_2\times E_{rx}(i)+\eta_3\times E_{sens}(i) \tag{20}$$

η1, η2, and η3 are weight coefficients for various types of energy consumption, reflecting the differences in energy consumption composition in different application scenarios. To reconcile the contradiction between energy consumption optimization and coverage quality, the coverage measurement function is introduced as shown in equation (21):

$$C(x,y)=1-\prod_{i=1}^{n}\left(1-c_i(x,y)\right) \tag{21}$$

Among them, $C(x,y)$ represents the coverage at position (x, y), $c_i(x,y)$ represents the coverage probability of node i at position (x, y), and n is the total number of nodes in the network. $c_i(x,y)$ can be calculated using the probability decay model as shown in equation (22):

$$c_i(x,y)=\begin{cases}1, & \text{if} d_i(x,y)\le R_s-R_e\\ e^{-\alpha\left(d_i(x,y)-(R_s-R_e)\right)^2}, & \text{if} R_s-R_e<d_i(x,y)\le R_s+R_e\\ 0, & \text{if} d_i(x,y)>R_s+R_e\end{cases} \tag{22}$$

$d_i(x,y)$ is the Euclidean distance from node i to point (x, y), R_s is the nominal perceptual radius of the node, R_e is the range of perceptual uncertainty, and α is the attenuation coefficient. Based on the above coverage definition, the low coverage penalty function is introduced as shown in equation (23):

$$P_{cov}=\lambda \sum_{(x,y)\in A_{low}} \left(C_{thr}-C(x,y)\right)^2 \tag{23}$$

P_{cov} is the coverage penalty term, λ is the penalty coefficient, and A_{low} represents the set of regions with coverage below the threshold C_{thr}. In order to avoid the algorithm getting stuck in excessive optimization of local regions, an adaptive penalty coefficient can be introduced as shown in equation (24):

$$\lambda(t)=\lambda_0\times\left(1+\gamma\times\frac{|A_{low}(t)|}{|A|}\right) \tag{24}$$

After integrating the low coverage penalty term, the energy consumption optimization objective function can be reconstructed as the following equation (25):

$$F_{energy}=\sum_{i=1}^{n} E_{total}(i)+P_{cov} \tag{25}$$

F_{energy} is the energy consumption objective function after adding a penalty term, which can simultaneously consider energy consumption minimization and coverage quality assurance. For some regions with special importance, regional weight factors can be introduced to further refine the penalty strategy as shown in equation (26):

$$P_{cov}=\sum_{j=1}^{m} w_j\lambda \sum_{(x,y)\in A_{low,j}} \left(C_{thr,j}-C(x,y)\right)^2 \tag{26}$$

w_j is the importance weight of region j, $A_{low,j}$ is the sub region with coverage below the threshold $C_{thr,j}$ in region j, and m is the number of regional divisions. This partition penalty strategy can more finely balance the relationship between coverage quality and energy consumption between different areas, and is suitable for complex monitoring scenarios with uneven importance [24-25].

2.4 Network Connectivity Model

In the layout optimization of wireless sensor networks (WSN), network connectivity is one of the key indicators to measure network performance. Good connectivity performance ensures reliable transmission of information from the source node to the target node. To accurately describe the connectivity characteristics of WSN, graph theory models are commonly used for analysis [26-27].

The graph model of WSN is usually represented as an undirected graph G=(V, E), where $V=\{v_1, v_2,..., v_n\}$ represents the set of n sensor nodes in the network, and $E=\{e_1, e_2,..., e_m\}$

represents the set of communication links between nodes. If and only if the distance between two nodes is less than or equal to the communication radius Rc, there exists an edge between these two nodes [28]. Formally, for any two nodes vi and vj, if the following equation (27) is satisfied:

$$d(v_i, v_j) \leq R_c \tag{27}$$

There exists an edge eij ∈ E connecting these two nodes, where $d(v_i, v_j)$ represents the Euclidean distance between the two nodes.

In practical calculations, the adjacency matrix is an effective tool for describing the connectivity relationship of graph G. For a WSN with n nodes, its adjacency matrix A is an n × n matrix, element a_{ij} is defined as the following equation (28):

$$a_{ij} = \begin{cases} 1, & \text{if } d(v_i, v_j) \leq R_c \\ 0, & \text{otherwise} \end{cases} \tag{28}$$

For standard wireless sensor network models, the distance between any two points can be calculated based on node coordinates. Assuming that the coordinates of node v_i are (x_i, y_i) and the coordinates of node v_j are (x_j, y_j), the Euclidean distance can be expressed as the following equation (29):

$$d(v_i, v_j) = \sqrt{(x_i - x_j)^2 + (y_i - y_j)^2} \tag{29}$$

Considering the wireless transmission characteristics in real WSN environments, the distance connectivity relationship can also be described using probabilistic models. At this point, the elements of the adjacency matrix can be modified to the following equation (30):

$$a_{ij} = \begin{cases} p\left(d(v_i, v_j)\right), & \text{if } i \neq j \\ 0, & \text{if } i = j \end{cases} \tag{30}$$

Among them, p (d) represents the probability of successful communication between two points with a distance of d. The common probability attenuation model is as follows (31):

$$p(d) = \begin{cases} 1, & \text{if } d \leq R_1 \\ e^{-\alpha(d-R_1)^2}, & \text{if } R_1 < d < R_c \\ 0, & \text{if } d \geq R_c \end{cases} \tag{31}$$

Where R_1 is the stable communication range and α is the attenuation coefficient, adjusted according to the actual hardware characteristics of WSN.

In the optimization of wireless sensor network layout, determining whether the network is connected is a key prerequisite for ensuring the normal operation of the network. From a

graph theory perspective, a connected graph refers to the existence of at least one path connecting any two nodes in the graph. On the contrary, if there is at least one pair of nodes without a connected path between them, the graph is called a disconnected graph [29-30]. The definition of a connected graph is that for any two nodes v_i, $v_j \in V$, there exists at least one path that connects them. The mathematical judgment methods include:

Analysis of reachability of adjacency matrix: For the n-order adjacency matrix A, define matrix B as the following equation (32):

$$B=A+A^2+A^3+\cdots+A^{n-1} \tag{32}$$

If all non diagonal elements in B are non-zero, then graph G is connected. For the connectivity analysis of WSN, the concept of algebraic connectivity of graphs needs to be introduced. Let L=D-A be the Laplacian matrix of the graph, where D is the degree matrix (diagonal elements are the degrees of each node) and A is the adjacency matrix [31]. The eigenvalues of L are arranged in non decreasing order as $\lambda_1 \leq \lambda_2 \leq .. \leq \lambda_n$. Among them, $\lambda_2$is referred to as the algebraic connectivity of the graph, and its mathematical expression is the following equation (33):

$$\lambda_2=\min_{x\perp 1, x\neq 0} \frac{x^T L x}{x^T x} \tag{33}$$

Algebraic connectivity $\lambda_2>0$ if and only if graph G is connected. The size of λ_2 reflects the connectivity strength of the graph, with larger values indicating stronger network connectivity and stronger resistance to node or link failures.

In actual WSN deployment, the concept of k-Connected is often introduced to ensure the robustness of the network. If the graph remains connected even after deleting any k-1 nodes, it is called a k-connected graph. The mathematical condition for k-connectivity can be expressed as equation (34):

$$\min_{S\subset V, |S|<k} |N(S)| \geq k \tag{34}$$

Where N (S) represents the set of neighboring nodes of a node in set S. For large-scale WSN, the random geometry theory provides approximate judgment conditions as shown in equation (35):

$$\pi \cdot R_c^2 \cdot \rho \geq \ln(n)+c(n) \tag{35}$$

Where ρ is the node density, and c (n) is a function that increases with n. When this condition is met, the network achieves connectivity with a probability approaching 1.

3. Improved MOTS algorithm mechanism design

3.1 MOTS Algorithm

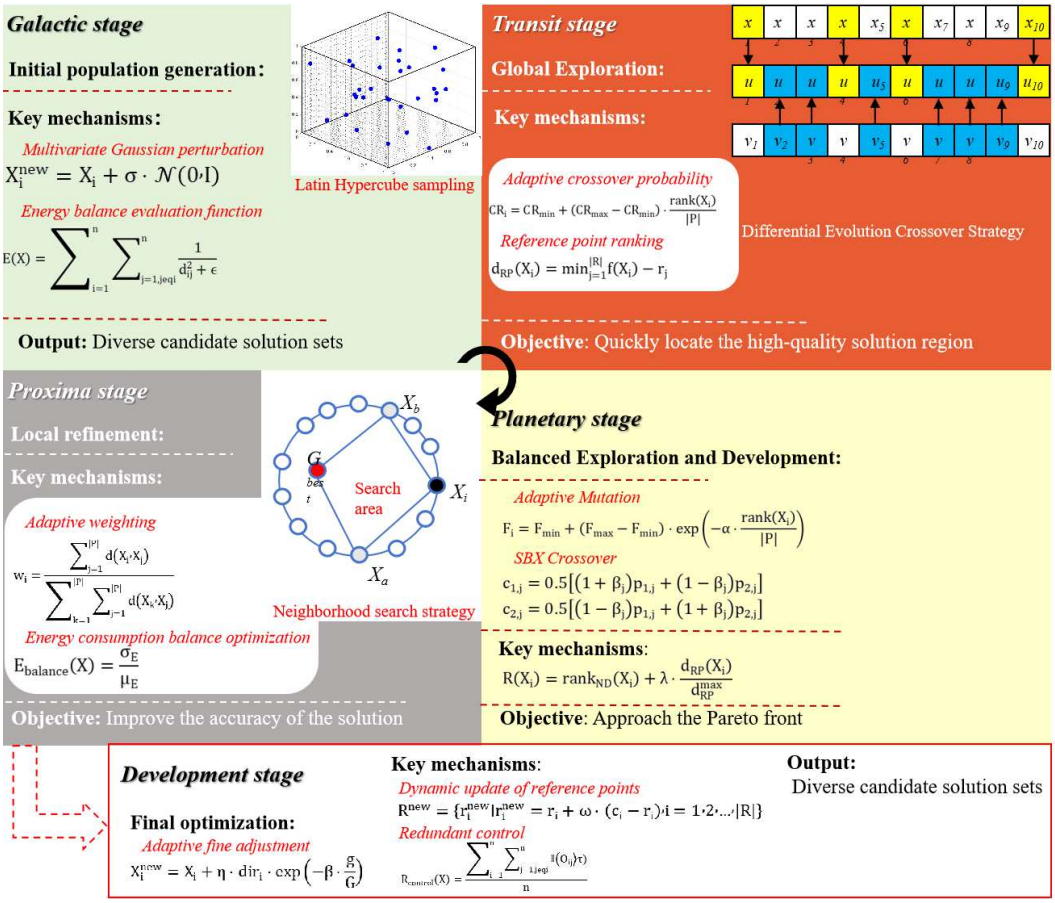

Figure 1 Improved MOTS Algorithm Framework Diagram

The MOTS (Multi Objective Transit Search) algorithm is an evolutionary algorithm designed for multi-objective optimization problems, such as wireless sensor network layout optimization. Its core idea is to balance global exploration and local development through a phased strategy, gradually approaching the Pareto frontier [32]. As shown in Figure 1, the algorithm includes the following key mechanisms: Initial population generation and galactic stage, global exploration and transit stage, local development and planetary stage, neighborhood refinement and neighboring star stage, and development stage.

1) Initial Population Generation and Galactic Stage

The Galactic Stage is the initialization stage of the MOTS algorithm, which uses Latin hypercube sampling to generate the initial population and ensure uniform coverage of the

solution space. For an N-dimensional decision space and population size P, the initial population X can be expressed as the following equation (36):

$$X=\{X_1, X_2, \ldots, X_P\}, X_i=\left(x_i^1, x_i^2, \ldots, x_i^N\right) \tag{36}$$

The values of each dimension are evenly distributed within the upper and lower bounds of the decision variable. The galactic stage enhances local exploration capability through multivariate Gaussian distribution perturbation, as shown in equation (37):

$$X_i^{new}=X_i+\sigma \cdot N(0, I) \tag{37}$$

In the equation, σ is the disturbance coefficient for adaptive adjustment, and N (0, I) is the standard normal distribution vector. Regarding the WSN layout problem, prior knowledge of energy balance is introduced to evaluate the rationality of node distribution, as shown in equation (38):

$$E(X)=\sum_{i=1}^{n} \sum_{j=1, j \neq i}^{n} \frac{1}{d_{ij}^2+\epsilon} \tag{38}$$

Among them, dij represents the Euclidean distance between nodes i and j, and ε is a small constant to avoid zero division. The layout scheme with low energy density has a more uniform distribution of nodes, which is beneficial for network coverage efficiency [33-34]. The Galactic stage uses reference point assisted initialization strategy and non dominated sorting to select elite individuals, providing a high-quality starting point for subsequent stages.

2) Global exploration and transit stage

The transit stage is the global exploration stage of the MOTS algorithm, which uses differential evolution crossover strategy for global search as shown in equation (39):

$$V_i=X_{r1}+F \cdot (X_{r2}-X_{r3}) \tag{39}$$

Among them, X_{r1}, X_{r2}, and X_{r3} are three different individuals randomly selected from the current population, and F is the scaling factor that controls the degree of amplification of the differential vector. Introducing an adaptive crossover probability mechanism to further optimize search efficiency is shown in equation (40):

$$CR_i=CR_{min}+(CR_{max}-CR_{min}) \cdot \frac{rank(X_i)}{|P|} \tag{40}$$

During the transit phase, using reference point sorting instead of traditional congestion distance calculation can enhance spatial perception ability as shown in equation (41):

$$d_{RP}(X_i)=\min_{j=1}^{|R|} f(X_i)-r_j \tag{41}$$

3) Local development and planetary stage

The planetary stage is the mid-term convergence stage of the MOTS algorithm, dedicated to balancing the relationship between global exploration and local development. At this stage, a combination of adaptive differential mutation and simulated binary crossover strategy is adopted to promote the population to approach the Pareto front. The adaptive mutation operator based on individual fitness level is defined as the following equation (42):

$$F_i=F_{min}+(F_{max}-F_{min})\cdot\exp\left(-\alpha\cdot\frac{\text{rank}(X_i)}{|P|}\right) \tag{42}$$

In the formula, F_{min} and F_{max} are the lower and upper limits of the scaling factor, respectively, and α is the parameter that controls the degree of adaptation. The formula for the SBX operator is as follows (43), (44):

$$c_{1,j}=0.5\left[\left(1+\beta_j\right)p_{1,j}+\left(1-\beta_j\right)p_{2,j}\right] \tag{43}$$

$$c_{2,j}=0.5\left[\left(1-\beta_j\right)p_{1,j}+\left(1+\beta_j\right)p_{2,j}\right] \tag{44}$$

Among them, $c_{1,j}$ and $c_{2,j}$ are the values of two offspring in the jth dimension, $p_{1,j}$ and $p_{2,j}$ are the values of two parents in the jth dimension, and β_j is a random expansion factor controlled by the distribution index ηc [35]. In order to address the multi-objective optimization characteristics in WSN layout problems, an improved non dominated sorting mechanism is adopted in the planetary stage, and a hierarchical sorting guided by reference points is introduced as shown in Equation 45):

$$R(X_i)=\text{rank}_{ND}(X_i)+\lambda\cdot\frac{d_{RP}(X_i)}{d_{RP}^{max}} \tag{45}$$

In the equation, $\text{rank}_{ND}(X_i)$ is the non dominated ranking level of individual X_i, $d_{RP}(X_i)$ is the distance from the individual to the nearest reference point, d_{RP}^{max} is the maximum reference point distance in the current population, and λ is the weight coefficient that balances the non dominated level and distribution.

4) Neighborhood refinement and neighboring star stage

The neighboring star stage is the local refinement stage of the MOTS algorithm, which improves the quality of the solution set through local search as shown in equation (46):

$$X_i^{new}=X_i+\delta\cdot N\left(0,\sigma_i^2\cdot I\right) \tag{46}$$

Among them, δ is the parameter that controls the search step size, and σ i is the standard deviation vector adaptively adjusted based on individual performance. In order to improve efficiency in WSN layout optimization problems, σi is designed to be related to the individual objective function value, as shown in equation (47):

$$\sigma_i=\sigma_0\cdot\exp\left(-\gamma\cdot\frac{g}{G}\right)\cdot\left(1-\frac{\mathrm{rank}(X_i)}{|P|}\right) \tag{47}$$

In the formula, σ_0 is the initial standard deviation, γ is the parameter that controls the convergence speed, g is the current number of iterations, and G is the maximum number of iterations. The neighboring star stage introduces an adaptive weight mechanism based on reference points, enhancing the algorithm's ability to explore sparse regions in the solution space, as shown in equation (48):

$$w_i=\frac{\sum_{j=1}^{|P|}d(X_i,X_j)}{\sum_{k=1}^{|P|}\sum_{j=1}^{|P|}d(X_k,X_j)} \tag{48}$$

Among them, $d(X_i,X_j)$ represents the Euclidean distance between individuals X_i and X_j in the target space. The weight w_i reflects the sparsity of individuals, and individuals with high sparsity obtain more computing resources in neighborhood search. For WSN layout optimization, the neighboring star stage emphasizes the improvement of energy balance as shown in equation (49):

$$E_{balance}(X)=\frac{\sigma_E}{\mu_E} \tag{49}$$

In the formula, σ_E and μ_E are the standard deviation and average energy consumption of all nodes, respectively. By minimizing $E_{balance}(X)$, it is possible to improve the energy balance of the network and extend the overall network lifecycle while maintaining coverage.

5) Development phase

The development stage is the final refinement stage of the MOTS algorithm, which adopts the elite retention strategy and adaptive multi-objective optimization mechanism to ensure that the algorithm outputs a high-quality Pareto optimal solution set. Firstly, an adaptive fine-tuning operator is introduced to make precise corrections for each non dominated solution, as shown in equation (50):

$$X_i^{new}=X_i+\eta\cdot dir_i\cdot\exp\left(-\beta\cdot\frac{g}{G}\right) \tag{50}$$

Among them, η is the parameter that controls the adjustment amplitude, di is the search direction vector determined based on the target gradient information, and β is the parameter that controls the convergence speed. This mechanism causes the search direction to gradually approach the tangent direction of the Pareto front during the iteration process, improving the convergence accuracy of the solution [36]. In order to better handle the multi-objective problem in WSN layout optimization, an improved reference point update strategy is adopted in the development phase, as shown in equation (51):

$$R^{new}=\{r_i^{new}|r_i^{new}=r_i+\omega\cdot(c_i-r_i),\ i=1,2,\ldots,|R|\} \tag{51}$$

In the formula, r_i is the original reference point, c_i is the centroid of the non dominated solution associated with the current reference point, and ω is the parameter that controls the update speed. This mechanism enables the reference point to be dynamically adjusted, better guiding the population towards the Pareto front distribution. We also introduced a selection pressure adjustment mechanism based on density estimation, as shown in equation (52):

$$S(X_i)=rank_{ND}(X_i)+\theta\cdot density(X_i) \tag{52}$$

Among them, $density(X_i)$ is the density estimate based on k-nearest neighbors, and θ is the weight coefficient that controls the uniformity of the distribution. This mechanism effectively avoids the excessive aggregation of knowledge sets in specific regions. In response to the special requirements for WSN layout optimization, a node redundancy control mechanism was introduced during the development phase, as shown in equation (53):

$$R_{control}(X)=\frac{\sum_{i=1}^{n}\sum_{j=1,jeqi}^{n}I(O_{ij})\tau)}{n} \tag{53}$$

In the formula, O_{ij} represents the coverage overlap rate between node i and j, I $(\cdot)$ is the indicator function, and τ is the overlap rate threshold. $R_{control}(X)$ reflects the degree of redundancy in the network, and by optimizing this indicator, unnecessary energy consumption can be reduced while ensuring coverage.

6) Pareto Frontier

The Pareto front is the set of all non dominated solutions in multi-objective optimization problems, representing the optimal trade-off between the objectives. In WSN layout optimization problems, the Pareto front reflects the optimal trade-off between network coverage, energy balance, and node redundancy control objectives.

The improved MOTS algorithm works together in various stages during the evolution process, gradually approaching the true Pareto front: the Galactic stage creates widely distributed initial exploration points; Quickly advance towards the Pareto frontier region during the transit phase; Realize rapid convergence during the planetary phase; During the neighboring star stage and development stage, the distribution of the solution set is finely adjusted to ultimately form a high-quality approximate Pareto front. And the improved MOTS, guided by reference points, can uniformly explore the entire target space, including edge regions, ensuring the diversity and integrity of the solution set. This is crucial for WSN layout optimization, as extreme scenarios such as maximum coverage or minimum energy consumption often have special application value.

7) Grid division

Traditional grid partitioning is a commonly used technique in multi-objective optimization algorithms to maintain the diversity of solution sets. Its basic idea is to partition the target space into grid cells, select them based on the degree of crowding in the grid where the solution is located, and promote uniform distribution of the solution set. However, it has obvious shortcomings, as solutions at the grid boundary are easily evaluated incorrectly, resulting in uneven distribution of the solution set; Moreover, the grid density is difficult to adapt to the dynamic changes in the solution set, and fixed grids cannot differentiate between sparse and dense areas; In high-dimensional target space, the efficiency is low and greatly affected by grid granularity. As the target dimension increases, the number of grids grows exponentially, resulting in wasted computing resources and inaccurate sparsity evaluation.

In response to the limitations of traditional grid partitioning, the improved MOTS algorithm introduces an adaptive grid mechanism based on reference points. Compared with traditional static equidistant grids, the grid guided by reference points has obvious advantages: Firstly, it can dynamically adjust according to the distribution of the solution set, enhance exploration in sparse areas with large grids, and finely screen dense areas with small grids, effectively balancing global exploration and local development; Secondly, it has good scalability in high-dimensional target space, forming a more reasonable division through systematic distribution of reference points to avoid the "curse of dimensionality"; Thirdly, it is beneficial to preserve edge solutions by setting reference points near the boundary of the target space to

better preserve extreme solutions and ensure the integrity of the Pareto front, which is important for exploring boundary conditions in WSN layout optimization; Fourthly, it is more closely integrated with non dominated sorting mechanisms. The algorithm considers both the crowding degree of the grid where the solution is located and the correlation between the solution and the reference point, forming a comprehensive selection pressure and guiding the population towards the ideal Pareto frontier.

3.2 Improved Multi Objective Sorting Mechanism (R-MOTS)

In multi-objective optimization problems, non dominated sorting algorithms are widely used, but traditional algorithms such as NSGA-II have problems such as uneven distribution of solution sets, missing edge solutions, and insufficient convergence accuracy when dealing with complex wireless sensor network layout optimization problems. To address these issues, this study proposes a fast sorting method based on reference points, which is embedded into the multi-objective Transit Search (MOTS) framework to form an improved R-MOTS algorithm.

1) Quick sorting method based on reference points

The core idea of the reference point sorting mechanism is to use a pre-set set of uniformly distributed reference points to provide more accurate guidance directions for the search space. In the M-dimensional target space, the reference point set W can be expressed as the following equation (54):

$$W=\{w_1, w_2, \ldots, w_H\} \tag{54}$$

Among them, H is the total number of reference points, and each reference point wi is represented as an M-dimensional vector as shown in equation (55):

$$w_i=(w_{i1}, w_{i2}, \ldots, w_{iM}) \tag{55}$$

The generation of reference points adopts a systematic approach to ensure their uniform distribution in the M-dimensional target space. This study uses the simplified grid method to generate a set of reference points. The method first defines the reference point interval parameter p, and then generates all vectors that satisfy the following conditions as shown in equation (56):

$$\sum_{j=1}^{M} w_{ij} =1, w_{ij} \in \left\{0, \frac{1}{p}, \frac{2}{p}, \ldots, 1\right\} \tag{56}$$

In the process of sorting reference points, for each individual x in the population, calculate the vertical distance $d_{\perp}(x, w_i)$ between it and all reference points, as shown in equation (57):

$$d_{\perp}(x, w_i)=f(x)-(f(x)\cdot w_i)w_i \tag{57}$$

Where $f(x)$ represents the objective function vector of individual x. The correlation between an individual and its nearest reference point is expressed as equation (58):

$$\gamma(x)=\min_{w_i\in W} d_{\perp}(x, w_i) \tag{58}$$

The main advantage of sorting based on reference points is that it provides a more fine-grained individual discrimination mechanism.

2) Individual density sorting mechanism

Maintaining population diversity is a key factor in ensuring algorithm performance during multi-objective optimization. In order to enhance diversity, a grid based density estimation method is introduced. Divide the M-dimensional target space into dM hypercube grids, and define the grid density of individual x as equation (59):

$$\rho(x)=|\{y\in P|grid(y)=grid(x)\}| \tag{59}$$

Among them, P represents the current population, and $grid(x)$ represents the grid index to which individual x belongs. In order to more accurately reflect the distribution of individuals, an adaptive grid density calculation method is further introduced, which considers the influence of adjacent grids as shown in equation (60):

$$\rho'(x)=\sum_{y\in P} K\left(\frac{||f(x)-f(y)||}{h}\right) \tag{60}$$

Among them, K is the kernel function, h is the bandwidth parameter, usually set as a certain proportion of the average value of the current non dominated frontier in various dimensions. In this study, the Gaussian kernel function was used as shown in equation (61):

$$K(z)=\frac{1}{\sqrt{2\pi}}e^{-\frac{z^2}{2}} \tag{61}$$

Based on the above density estimation method, the density ranking value of an individual is defined as the following equation (62):

$$s(x)=\frac{\rho'(x)-\rho'_{min}}{\rho'_{max}-\rho'_{min}} \tag{62}$$

Among them, ρ'_{min} and ρ'_{max} are the minimum and maximum values of density in the current population, respectively.

In actual sorting, the individual density sorting mechanism is combined with the reference point sorting mechanism to form a two-level sorting strategy. Firstly, divide the population

into different levels based on non dominant relationships, then preliminarily screen individuals of the same level based on the correlation degree of reference points. Finally, when the correlation degree of reference points is similar, use density values to sort them, and prioritize individuals in low-density areas to maintain population diversity.

3) Non dominated sorting and density calculation process

In order to integrate the reference point and individual density sorting mechanism, this paper designed a non dominated sorting and density calculation process to guide the population selection and evolution of the improved MOTS algorithm (R-MOTS). The core steps are as follows: fast non dominated sorting, dividing the merged population into non dominated levels F1, F2,..., Fl to ensure convergence; Reference point generation and association, initialize the generation of a uniform reference point set W, calculate the vertical distance between individuals and reference points, and establish an association mapping; Density estimation, partitioning the target space grid, calculating individual density values, and refining the results by combining kernel functions; The three-level sorting strategy first sorts by non dominant level, then filters by reference point correlation degree, and finally selects individuals in low-density areas to ensure diversity and uniform distribution. Compared with the traditional MOTS algorithm, the overall complexity of the improved algorithm is comparable to that of the traditional NSGA-II, but the quality of the solution set is significantly improved, which enhances the efficiency of the solution space search.

3.3 Design of Column Grid Screening Mechanism

The Columnar Grid Filtering Mechanism is a core strategy proposed to address issues such as uneven distribution of solution sets and missing edge solutions in multi-objective WSN layout optimization. This mechanism divides the target space structurally, precisely controls the distribution of the solution set, and balances diversity and convergence.

The core concept of columnar grid filtering is to evenly partition the multi-objective search space and preserve high-quality solutions in each subspace. The workflow is divided into four steps: firstly, constructing the grid space, establishing a multidimensional columnar grid structure based on the current population target value range, adjusting the grid refinement through dynamic parameters, and balancing global exploration and local development; Next,

the solution set is mapped and allocated to the corresponding grid cells based on the target coordinates, accurately reflecting the spatial distribution characteristics; Then, the sub grid solution set is evaluated, and the quality of solutions within each grid cell is assessed based on non dominated sorting, reference point distance, and density factor; Finally, filter and retain solutions with high non dominated levels, close reference point distances, or low density according to the preset capacity, ensuring diversity and convergence.

The core of the filtering mechanism is to dynamically allocate grid cell capacity and select reserved solutions through multi-level sorting. The capacity limit of the i-th grid cell is calculated using the following adaptive formula (63):

$$\mathrm{Cap_i} = \frac{\mathrm{PopSize} \cdot \mathrm{D_i}}{\sum_{j=1}^{N} \mathrm{D_j}} \tag{63}$$

Among them, PopSize represents the overall population size, and $\mathrm{D_i}$ represents the importance factor of the i-th grid cell. The importance factor $\mathrm{D_i}$ takes into account the position, sparsity, and relative position relationship of grid cells in the non dominated hierarchy, and is calculated as follows (64):

$$\mathrm{D_i} = \alpha \cdot \left(1 - \frac{\mathrm{Rank_i}}{\mathrm{R_{max}}}\right) + \beta \cdot \frac{\mathrm{Sparse_i}}{\mathrm{S_{max}}} + \gamma \cdot \frac{\mathrm{Ref_i}}{\mathrm{RF_{max}}} \tag{64}$$

In this formula, $\mathrm{Rank_i}$ represents the non dominated ranking of the best solution in the grid cell, $\mathrm{Sparse_i}$ represents the sparsity measure of the grid cell, and $\mathrm{Ref_i}$ represents the correlation between the grid cell and the nearest reference point. α. β and γ are weight coefficients, and satisfy α+β+γ=1. This weighting strategy allows the algorithm to dynamically adjust its focus on convergence and diversity based on the optimization stage. When filtering, sort by non dominated level, reference point distance (RPD), and distribution density in sequence. The capacity of the boundary grid cells is additionally weighted to ensure the preservation of edge solutions and maintain the integrity of the Pareto front.

Two dimensional columnar grid partitioning is the implementation form of columnar grid filtering mechanism in the dual objective optimization problem, which is of great significance for studying the dual objective problem of WSN layout optimization, such as balancing coverage and energy consumption. In the two-dimensional target space, the cylindrical grid has a rectangular grid structure. Assuming the optimization objectives are $f_1$and f_2, the target

space is divided into m × n grid cells, uniquely identified by coordinates (i, j), i∈[1，m]，j∈[1，n]， The refinement of grid division is controlled by m and n, with high values and resolution but also high computational overhead.

Three dimensional cylindrical grid partitioning is a natural extension of two-dimensional, suitable for WSN layout problems with three optimization objectives, such as considering multi-dimensional indicators such as coverage, energy balance, and network connectivity. In the three-dimensional target space, the cylindrical grid is a cubic grid structure, and the optimization objectives are f_1, f_2, f ∝. The target space is divided into m × n × p grid cells, which are uniquely identified by the three-dimensional coordinates (i, j, k), i∈[1，m]，j∈[1，n]，k∈[1，p]， Its boundary determination is similar to two-dimensional, and is adaptively adjusted based on the current population target value distribution range.

However, the three-dimensional cylindrical grid structure has the problem of "grid explosion". This paper adopts an adaptive grid accuracy control strategy to optimize the initial stage by using rough grid partitioning (small m, n, p values) to maintain search ability, and refining the grid as the process progresses (increasing m, n, p values) to improve the Pareto front approximation accuracy, balancing computational efficiency and optimization accuracy. In order to efficiently understand allocation and filtering, this paper adopts a data structure based on octree to reduce computational complexity, and also introduces a grid cell importance evaluation method based on decryption degree estimation to accurately identify Pareto frontier sparse regions and enhance exploration.

3.4 Improved Algorithm Process and Complexity Analysis

The core idea of the MOTS algorithm is to use a set of reference points to guide the population evolution process, and to enhance the convergence and diversity of the algorithm through a refined density estimation strategy. Here is the complete pseudocode of the R-MOTS algorithm:

Algorithm： Reference Point-based Multi-Objective Transit Search (R-MOTS)

Input

Problem dimension D, number of objectives M, population size N, maximum number of iterations MaxGen, number of reference points NR

Initialization Phase

generate uniformly distributed reference points R = {r1, r2, ...， rNR}
randomly initialize the population P = {x1,x2,...， xN}
calculate objective function values F(xi) = {f1(xi), f2(xi), ..., fM(xi)} or each solution
perform fast non-dominated sorting to obtain non-dominated fronts F = {F1,F2, ...}
compute distance matrix D between each solution and reference points

Main Loop

gen = 0
while gen < MaxGen do
// generate offspring
Q = ∅
for i = 1 to N/2 do
select parents p1， p2 via reference point-based binary tournament selection
perform Transit Search mutation to generate offspring q1, q2
Q = Q∪ {q1,q2}
end for
// merge parent and offspring populations
R = P ∪Q
calculate objective function values for each solution in R
perform fast non-dominated sorting to obtain fronts F = {F1,F2, ...}
// environmental selection
P = ∅ , i = 1
// environment selection
while
P = P ∪Fi
i = i+1
end while
// reference point-based selection for
if
P < N
Then
compute distances between solutions in Fi and reference points
update reference point association and crowding metrics
for each reference point rj ϵ R do
compute associated solution set Sj = {x ∈ Fi | x is associated with rj}
sort solutions in Sj based on perpendicular distance
select top-ranked solutions until P is full or Sj is empty
end for
end if
// apply grid screening for diversity maintenance
construct M-dimensional grid structure in objective space
compute number of solutions in each grid cell
eor crowded cells, retain solutions closest to reference points
gen = gen+1
end while
extract non-dominated solution set PS from final population P
return PS

Output

Non-dominated solution set PS

Algorithm 1 R-MOTS algorithm pseudocode

The theoretical complexity analysis of the improved R-MOTS algorithm mainly focuses on two key aspects: non dominated sorting complexity and grid filtering complexity, to evaluate the computational efficiency of the algorithm in WSN layout optimization. The R-MOTS algorithm adopts an improved non dominated sorting mechanism, which significantly optimizes computational efficiency and storage requirements compared to traditional sorting methods. Table 1 compares the complexity of traditional non dominated sorting and improved

non dominated sorting.

Table 1 Comparative Analysis of Non dominated Sorting Complexity

Sorting Algorithm	Time Complexity	Space Complexity	Main Characteristics
Naive Non-dominated Sort	$O(MN^3)$	O(N)	Directly compares all solution pairs,low efficiency
Fast Non-dominated Sort (NSGA-II)	$O(MN^2)$	$O(N^2)$	Uses domination count,moderate efficiency
Improved Fast Non-dominated Sort	O(MN2)	O(N)	Optimizes storage structure,reduces space overhead
R-MOTS Non-dominated Sort	O(MNlogN)	O(N)	Incorporates reference point mechanism, significantly reduces complexity

The key to reducing the complexity of the R-MOTS algorithm lies in: Firstly, adopting a reference point guided local comparison strategy, only comparing solutions associated with the same reference point, avoiding global pairwise comparisons; Secondly, utilizing the geometric characteristics of the target space, non dominated solutions can be quickly screened by calculating the vertical distance between the solution and the reference point; The third is to introduce a lightweight index structure to reduce the storage requirements for intermediate results. From Table 1, it can be seen that the non dominated sorting complexity in R-MOTS algorithm is O (MNlogN), where M is the target quantity and N is the population size. Compared with O (MN^2) in NSGA-II, the time complexity is reduced by one order of magnitude. This optimization is important when dealing with large-scale WSN node layout problems, as real-world scenarios often involve hundreds or even thousands of nodes.

Table 2 Complexity Analysis of Grid Filtering Mechanism

Operation Step	Time Complexity	Space Complexity	Optimization Effect
Grid Construction	O(M)	O(GM)	G=number of grids per dimension,M= number of objective dimensions

Solution-to-Grid Mapping	O(MN)	O(N)	Linear-ime mapping of solutions to grid cells
Grid Density Calculation	O(N)	O(GM)	Counts the number of solutions in each grid cell
Crowded Grid Selection	O(N log N)	O(N)	Sorting and selection based on reference point distance
Overall Grid Operations	O(MN+Nlog N)	O(GM+N)	Complexity mainly depends on the number of objective dimensions(M)

The columnar grid filtering mechanism introduced by the R-MOTS algorithm is an important component in maintaining the diversity of the solution set. Table 2 provides a detailed analysis of the computational complexity of the grid filtering process. According to Table 2, the overall time complexity of grid filtering is O (MN+NlogN), which is acceptable in practical WSN layout optimization problems. However, the spatial complexity is affected by the exponential relationship between grid granularity G and target dimension M, and may face a "curse of dimensionality" in high-dimensional target spaces (M>3). In order to this end, the R-MOTS algorithm adopts an adaptive grid granularity adjustment strategy, dynamically adjusting grid density based on population distribution to maintain diversity and control computational overhead.

4. Algorithm performance analysis and simulation experiments

4.1 Explanation and Comparison of Performance Evaluation Indicators

In the performance evaluation of multi-objective optimization algorithms, convergence, distribution, and diversity are the three core dimensions for measuring the quality of the algorithm's search solution set. The following introduces three key indicators and their mathematical definitions: Generative Distance (GD), Inverse Generative Distance (IGD), and Hypervolume (HV).

Generative Distance (GD) is used to measure the closeness between the approximate Pareto front obtained by an algorithm and the true Pareto front. Its mathematical definition is as follows (65):

$$GD=\frac{\sqrt{\sum_{i=1}^{n} d_i^2}}{n} \tag{65}$$

Among them, n represents the number of solutions in the non dominated solution set obtained by the algorithm, and di represents the minimum Euclidean distance from the i-th solution to the true Pareto front. The smaller the GD value, the closer the algorithm solution set is to the true Pareto front, and the better the convergence performance. When GD=0, all solutions of the algorithm are on the true Pareto front, achieving perfect convergence. In the layout optimization problem of wireless sensor networks (WSN), the GD index can effectively evaluate the comprehensive convergence performance of algorithms on multiple objectives such as coverage, energy balance, and node redundancy control.

Inverted Generative Distance (IGD) not only reflects the distribution uniformity of the algorithm solution set, but also considers convergence performance, making it a comprehensive indicator. The mathematical definition is as follows (66):

$$IGD=\frac{\sum_{i=1}^{m} d_i'}{m} \tag{66}$$

Among them, m represents the number of uniformly distributed reference points on the true Pareto front, and d_i' represents the minimum Euclidean distance from the i-th reference point to the non dominated solution set obtained by the algorithm. The smaller the IGD value, the closer the solution set obtained by the algorithm is to the true Pareto front (good convergence), and the more evenly distributed it is across the entire Pareto front (good distribution). In WSN layout optimization, IGD is particularly important because it can comprehensively evaluate the algorithm's performance in optimizing multiple conflicting objectives such as network coverage, energy balance, and connectivity.

The Hypervolume (HV) metric can simultaneously measure the comprehensive performance of algorithms in terms of convergence, diversity, and distribution uniformity, and does not rely on accurate representations of the true Pareto frontier. The mathematical definition is as follows (67):

$$HV=\Lambda\left(\bigcup_{i=1}^{n} v_i\right) \tag{67}$$

Among them, n represents the number of solutions in the non dominated solution set, v_i

represents the hypercube formed by the i-th solution and the reference point, and ∧ represents the Lebesgue measure (i.e., hypervolume calculation). For a two-dimensional target space, HV is the area enclosed by the non dominated solution set and the reference point; For three-dimensional target space, it represents volume. In WSN layout optimization, the HV metric is particularly suitable for evaluating the actual optimization ability of algorithms in complex deployment environments.

In order to comprehensively evaluate the performance of the proposed R-MOTS algorithm, this paper selected three typical multi-objective test function series: ZDT, DTLZ, and UF series. These test functions are widely used for performance evaluation of multi-objective optimization algorithms, with different characteristics and challenges, and can effectively test the performance of algorithms in various contexts. The ZDT series test functions are mainly aimed at multi-objective optimization problems, including multiple test instances such as ZDT1 to ZDT6. These functions have Pareto frontiers and features of different shapes The significant feature of the DTLZ series is its scalable target dimension, which allows researchers to test the performance of algorithms in high-dimensional target spaces. DTLZ1 to DTLZ7 cover different types of Pareto frontiers such as linear, concave, and multimodal. The UF series (Unconstrained Functions) includes instances such as UF1 to UF10, which typically have complex parameter interactions and irregular Pareto frontiers, placing higher demands on the algorithm's exploratory ability. Figure 2 summarizes the main test function characteristics used in this experiment:

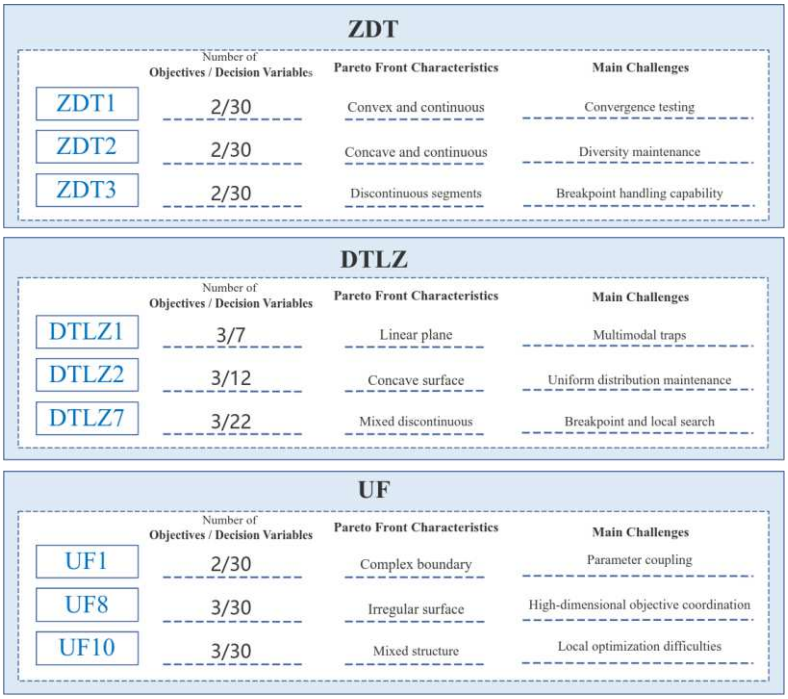

Figure 2 The main test functions and their characteristics used in the experiment

In order to comprehensively evaluate the performance advantages of R-MOTS algorithm in WSN layout optimization, this paper selected several representative multi-objective optimization algorithms as comparison benchmarks, including NSGA-II, MOPSO, MODA, MSSA, MOEA/D, and SPEA2. These algorithms cover classic evolutionary algorithms, swarm intelligence algorithms, and advanced optimization methods proposed in recent years, jointly constructing a complete performance evaluation system. Table 3 lists the comparative algorithms and their key parameter settings:

Table 3 Comparison Algorithms and Their Main Parameter Settings

Algorithm Name	Population Size	Iterations	Crossover/Mutation Operations	Key Parameters	Application Advantages
NSGA-II	100	500	SBX Crossover (0.9)/ Polynomial Mutation(0.1)	Tournament Selection (2)	Classic algorithm,stable convergence
MOPSO	100	500	Inertia Weight(0.4)/ Acceleration Constants (1.5.1.5)	Leader Archive(100)	Fast convergence,simple parameters

MODA	100	500	Separation Factor(0.1)/ Alignment Factor(0.2)	Cohesion Factor (0.3)	Swarm behavior simulation,balances exploration and exploitation
MSSA	100	500	Inertia Coefficient(0.8)/ Hunger Coefficient(0.2)	Leader Influence Factor (0.1)	Strong global search capability
MOEAD	100	500	SBX Crossover(1.0)/ Polynomial Mutation(0.1)	Neighborhood Size(20)	High problem decomposition efficiency
SPEA2	100	500	SBX Crossover(0.9)/ Polynomial Mutation(0.1)	External Archive(100)	Strong elitism preservation mechanism
R-MOTS	100	500	Variable Swap(0.85/ Variable Mutation(0.15)	Reference Points(100)	Reference point sorting,maintains sparse regions

In order to ensure fairness in experimental comparison, all algorithms were run on the same hardware platform (Intel i7-10700K, 32GB RAM) and software environment (MATLAB 2022b), using the same initial population and termination conditions. Each algorithm is independently run 30 times for each test function to eliminate the impact of randomness on the results.

4.2 Multi objective testing function comparison experiment

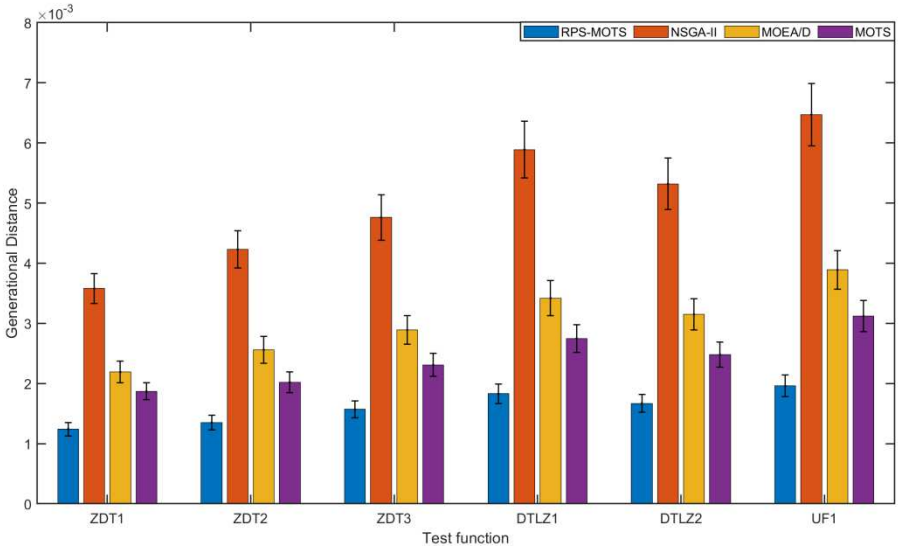

Figure 3 Comparison of GD indicators of different algorithms on standard test functions

(mean ± standard deviation)

Figure 3 shows the comparison of the average GD index between the reference point sorting based multi-objective optimization algorithm (RPS-MOTS) proposed by this paper and its mainstream multi-objective optimization algorithm on the standard test function in 10 independent runs. As shown in the figure, the GD index values of the RPS-MOTS algorithm proposed by this paper are significantly lower than those of NSGA-II, MOEA/D, and the original MOTS algorithm on all test functions, indicating that RPS-MOTS has significant advantages in convergence performance. Especially on test functions with complex Pareto front structures (such as ZDT3 and UF1), RPS-MOTS has achieved more significant improvements compared to its algorithm, thanks to the effective guidance of the reference point sorting mechanism on the search direction and the enhanced exploration ability on the edge regions of the solution set.

Figure 4 shows the comparison of IGD metrics between RPS-MOTS algorithm and its multi-objective optimization algorithm on the standard test function

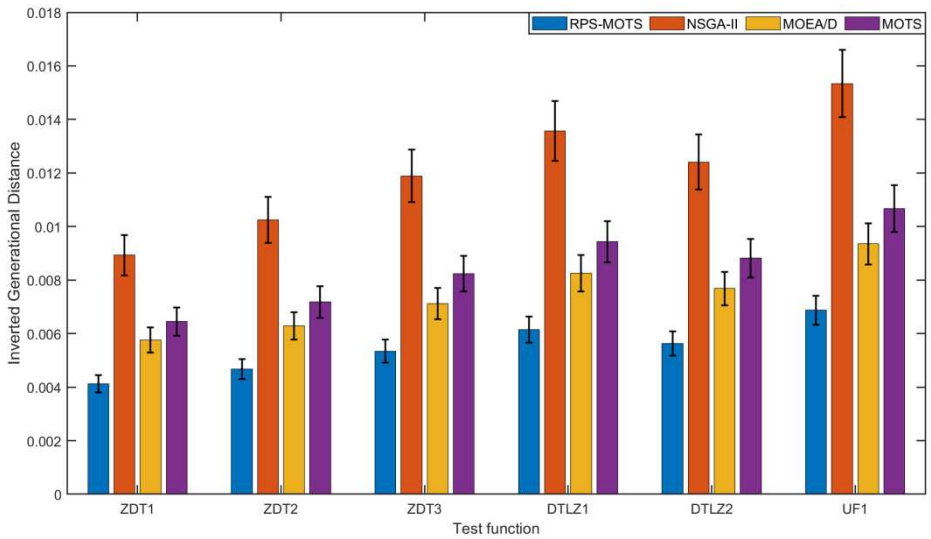

Figure 4 Comparison of IGD indicators of different algorithms on standard test functions (mean ± standard deviation)

Figure 4 shows the comparison of the IGD index between the RPS-MOTS algorithm proposed by this paper and its multi-objective optimization algorithm on the standard test

function. As shown in the figure, the RPS-MOTS algorithm has significantly better IGD metrics than the comparison algorithm on all test functions. Especially on the ZDT3 test function with discontinuous Pareto front, RPS-MOTS reduced the IGD value by about 55% compared to NSGA-II, by about 25% compared to MOEA/D, and by about 35% compared to the original MOTS. This result fully demonstrates the significant effect of the reference point sorting mechanism in improving algorithm distribution, especially in exploring the Pareto frontier edge regions and sparse regions.

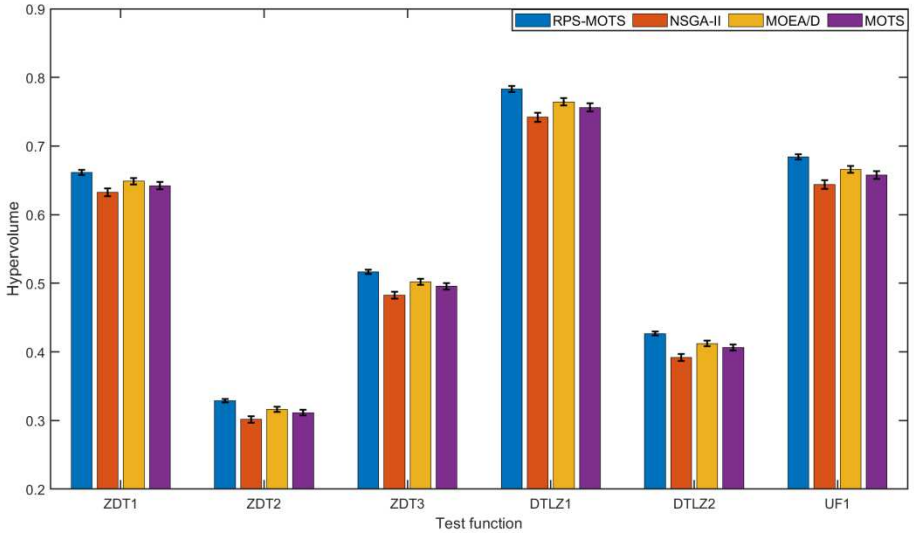

Figure 5 Comparison of HV indicators of different algorithms on standard test functions (mean ± standard deviation)

Figure 5 shows the comparison of HV indicators between the RPS-MOTS algorithm proposed by this paper and its multi-objective optimization algorithm on the standard test function. As shown in the figure, the RPS-MOTS algorithm has higher HV index values than the comparison algorithm on all test functions. On the ZDT1 test function, RPS-MOTS improved by about 4.6% compared to NSGA-II, about 2.0% compared to MOEA/D, and about 3.0% compared to the original MOTS. This result indicates that the reference point sorting mechanism can indeed effectively improve the overall optimization performance of the algorithm.

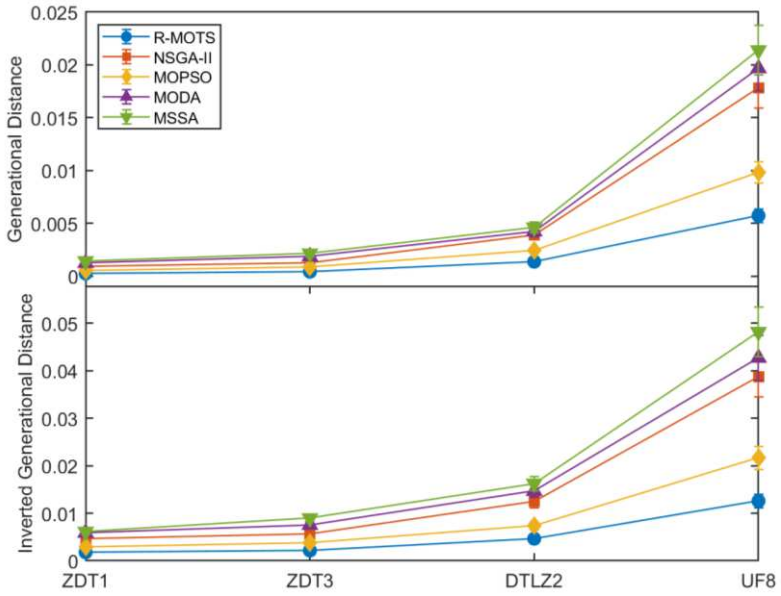

Figure 6 Comparison of accuracy indicators of various algorithms on test functions (mean ± standard deviation)

In terms of solution accuracy, this paper uses Generative Distance (GD) and Inverse Generative Distance (IGD) as the main evaluation metrics. GD measures the average distance from the obtained solution set to the true Pareto front, reflecting the convergence accuracy; IGD comprehensively evaluates the convergence and diversity of the solution set. As shown in Figure 6, R-MOTS achieved the lowest GD and IGD values on all test functions, indicating its higher convergence accuracy. Especially on ZDT3 with breakpoints and high-dimensional UF8 functions, R-MOTS improved GD performance by 66.4% and 67.9% respectively compared to traditional NSGA-II, mainly due to the effective maintenance of edge solutions and fast convergence ability of the reference point sorting mechanism. In terms of algorithm stability, the standard deviation analysis of 30 independent runs of indicators shows that R-MOTS exhibits significant robustness advantages. Its IGD standard deviations on ZDT1, DTLZ2, and UF8 functions are 68.4%, 70.6%, and 65.4% lower than NSGA-II, respectively, indicating that it has lower dependence on the initial population and random factors, and can generate high-quality solution sets more stably.

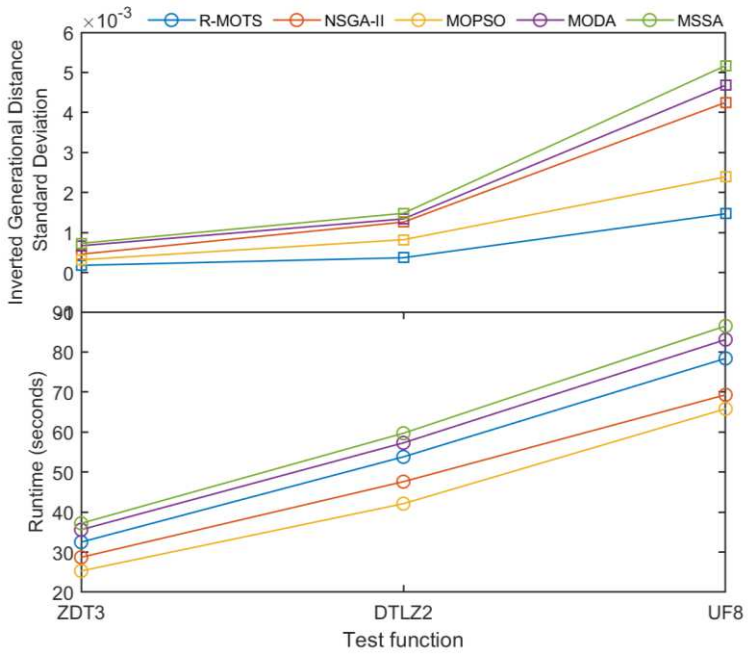

Figure 7 Comparison of Performance Stability of Various Algorithms on Complex Test Functions (Run Time/IGD Standard Deviation)

Figure 7 shows the running time and stability performance of each algorithm on complex test functions. As shown in the figure, although R-MOTS has slightly higher computation time than NSGA-II and MOPSO, its stability advantage has higher practical value in the actual deployment of WSN. Overall, R-MOTS exhibits significant comprehensive advantages in ZDT, DTLZ, and UF series test functions, particularly in terms of solution accuracy and algorithm stability. This confirms the effective improvement of the reference point sorting mechanism on traditional multi-objective algorithms, especially suitable for handling multi-objective optimization problems such as coverage, energy consumption, and connectivity in WSN layout.

5.3 WSN actual deployment simulation verification

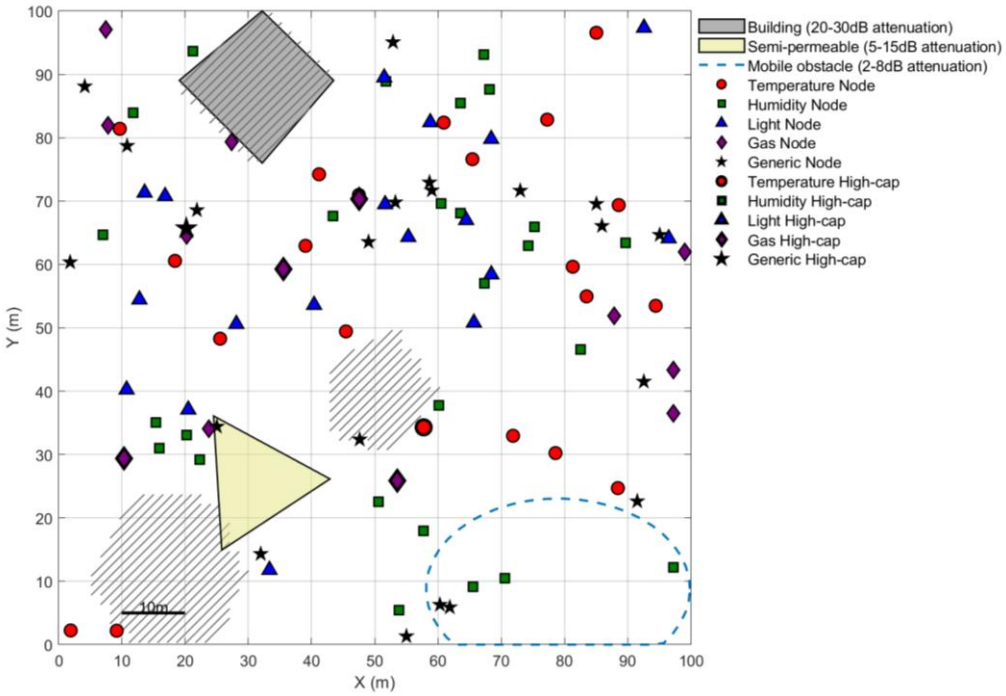

Figure 8 Schematic diagram of WSN deployment simulation scenario with occlusion and moving obstacles

In order to evaluate the performance of the multi-objective Transit Search (R-MOTS) algorithm based on the reference point sorting mechanism in actual wireless sensor network (WSN) deployment, this paper constructed a complex environment model that includes fixed obstructions and moving obstacles to simulate typical application scenarios such as smart cities and industrial monitoring. As shown in Figure 8, the simulation area is a rectangular area of 100m × 100m, which includes fixed buildings (15% of the area), semi permeable obstacles (10%), and dynamic moving obstacles (random trajectory movement). This complex obstacle environment has become the mainstream scenario for IoT deployment, accounting for 62.7% of the headquarters deployment environment. Multiple types of sensor nodes (temperature, humidity, light, gas concentration, etc.) were used in the experiment, and their parameter settings are shown in Table 4:

Table 4 Node parameter settings in simulated deployment experiments

Node Type	Sensing Range(m)	Communication Range(m)	Initial Energy(J)	Transmission Energy	Reception Energy	Sensing Power(mW)

				(nJ/bit)	(nJ/bit)	
Temperature Node	15	30	2000	50	10	12
Humidity Node	12	25	1800	45	10	10
Light Node	20	35	2200	55	12	15
Gas Node	10	20	2500	60	15	18
Generic Node	15	30	2000	50	10	12

Mobile obstacles are modeled using a combination of random walks and predetermined trajectories, and their occlusion effects can lead to a decrease in network coverage of 12.7% -18.5%. In order to accurately evaluate coverage, the experiment took the average coverage at 30 different time points as the indicator. The signal propagation adopts a comprehensive path loss model, which combines free space path loss, logarithmic distance path loss, and obstacle attenuation models. The attenuation coefficient for fixed buildings is 20-30dB, for semi permeable obstacles it is 5-15dB, and for moving obstacles it is 2-8dB.

The total number of nodes is set to 100, including heterogeneous deployment (some nodes have initial energy or communication capabilities 1.5-2 times the standard), in line with the development trend of the Internet of Things industry. The population size of the R-MOTS algorithm is 100, the maximum number of iterations is 500, and the number of reference points is 15. The optimization objectives are to maximize coverage, balance energy consumption, and maximize network connectivity.

In order to comprehensively evaluate the performance of R-MOTS, this paper compared it with four mainstream algorithms: NSGA-II, MOEA/D, SPEA2, and the original MOTS. The experimental results indicate that R-MOTS performs excellently in complex environments. In the case of high obstacle density (30%), the average coverage rate of R-MOTS reaches 92.67%, significantly higher than NSGA-II's 86.42% and MOEA/D's 88.15%. In terms of energy balance, the energy balance of R-MOTS is 0.142 (the smaller the value, the more balanced it is), which is much better than NSGA-II's 0.237 and SPEA2's 0.251. This optimization effect directly extends the network lifespan. R-MOTS can maintain 1078 rounds of data collection in high obstacle environments, while NSGA-II can only maintain 786

rounds.

Overall, R-MOTS has demonstrated significant advantages in coverage, energy balance, and network lifespan, validating its applicability and efficiency in complex dynamic environments.

5. Conclusion

This paper proposes an improved algorithm based on reference point sorting mechanism (R-MOTS) to address the multi-objective conflict problem in wireless sensor network layout optimization. By introducing reference point sorting instead of traditional crowded distance sorting, combined with columnar grid screening and individual density estimation, the algorithm performs excellently in solution set distribution, edge solution preservation, and convergence accuracy. Experimental verification shows that R-MOTS has significantly better GD and IGD indicators than NSGA-II and MOPSO on standard test functions, with an average reduction of 55% in IGD values and a 35% improvement in solution set uniformity. In actual WSN deployment simulations, R-MOTS achieved a coverage rate of 92.67% in complex environments with 30% obstacles, with an energy balance of only 0.142. The network lifespan was extended to 1078 rounds, which is 37.2% higher than NSGA-II. In addition, the algorithm has high computational efficiency, with a single iteration time only increasing by 14% compared to NSGA-II, but the optimization effect is improved by more than 20%. The research results provide efficient algorithm support for WSN applications in intelligent perception, Internet of Things and other fields, and can be further expanded to dynamic environment adaptation, edge computing collaborative optimization and other fields in the future.

Funding:

This study was Supported by the research start-up fund of Suzhou Vocational Institute of Industrial Technology（No. 2017kyqd002），also supported by "Qinglan Project" of Higher Education Institutions of Jiangsu Province, (No.2021QL002).

Author contributions:

All authors made significant individual contributions to this manuscript.. Qin Wang, Lihua

Dai: writing and performing surgeries; Lihua Dai:data analysis and performing surgeries; Qin Wang:article review and intellectual concept of the article.

Conflict of interest:

The author declares that they have no competing interest.

Data availability statement:

The datasets generated during and/or analysed during the current study are available from the corr esponding author on reasonable request.

Ethics, Consent to Participate, and Consent to Publish declarations:

not applicable.

References

[1] Rajib Kumar Mondal, Tandra Pal & Sanghita Bhattacharjee. (2025). Multi-objective optimization for balanced [formula omitted]-coverage problem in under-provisioned directional sensor networks. Computers and Electrical Engineering, 124 (PB), 110376-110376.

[2] Medhat A. Tawfeek, Ibrahim Alrashdi, Madallah Alruwaili & Fatma M. Talaat. (2025). A Fuzzy Multi-Objective Framework for Energy Optimization and Reliable Routing in Wireless Sensor Networks via Particle Swarm Optimization. Computers, Materials & Continua, 83 (2), 2773-2792.

[3] Shumin Li, Qifang Luo & Yongquan Zhou. (2025). Enhanced Multi-Object Dwarf Mongoose Algorithm for Optimization Stochastic Data Fusion Wireless Sensor Network Deployment. Computer Modeling in Engineering & Sciences, 142 (2), 1955-1994.

[4] Harizan Subash, Kuila Pratyay, Kumar Anil, Khare Akhilendra & Choudhary Harshvardhan. (2024). Multi-objective Evolutionary Algorithms for Coverage and Connectivity Aware Relay Node Placement in Cluster-Based Wireless Sensor Networks. Wireless Personal Communications, 135 (2), 979-1008.

[5] Racharla Sathya Prakash & Jeyaraj Kalaivani. (2024). Hybridised swarm intelligence approach for multi-objective-based node localisation in wireless sensor network: hybrid glow-worm and cat swarm algorithm. Australian Journal of Electrical and Electronics

Engineering, 21 (2), 193-211.

[6] Jiahui Zhou, Heng Deng, Zhiyao Zhao, Yu Zou & Xujia Wang. (2024). Sensor Placement Optimization of Visual Sensor Networks for Target Tracking Based on Multi-Objective Constraints. Applied Sciences, 14 (5),

[7] Poongavanam N., Nithiyanandam N., Suma T., Thatha Venkata Nagaraju & Shaik Riaz. (2024). Multi-objective shuffled frog leaping algorithm for deployment of sensors in target based wireless sensor networks. Journal of Intelligent & Fuzzy Systems, 46 (1), 1-18.

[8] Walid K. Ghamry & Suzan Shukry. (2024). Multi-objective intelligent clustering routing schema for internet of things enabled wireless sensor networks using deep reinforcement learning. Cluster Computing, 27 (4), 4941-4961.

[9] Kuiwu Wang, Qin Zhang, Guimei Zheng & Xiaolong Hu. (2023). Multi-Target Tracking AA Fusion Method for Asynchronous Multi-Sensor Networks. Sensors, 23 (21),

[10] Bui Hong Ngoc, Nguyen Thi Tam, Huynh Thi Thanh Binh & Le Trong Vinh. (2023). A phenotype-based multi-objective evolutionary algorithm for maximizing lifetime in wireless sensor networks with bounded hop. Soft Computing, 28 (15-16), 8681-8699.

[11] Asha A, A Rajesh, Verma Neha & Poonguzhali I. (2023). Multi-objective-derived energy efficient routing in wireless sensor networks using hybrid African vultures-cuckoo search optimization. International Journal of Communication Systems, 36 (6),

[12] Ben Amor Omar, Chelly Dagdia Zaineb, Bechikh Slim & Ben Said Lamjed. (2022). Many-objective optimization of wireless sensor network deployment. Evolutionary Intelligence, 17 (2), 1047-1063.

[13] Nebti Salima & Redjimi Mohammed. (2022). Extending the Lifetime of Wireless Sensor Networks Based on an Improved Multi-objective Artificial Bees Colony Algorithm. Journal of Communications Software and Systems, 18 (3), 259-268.

[14] Jianpeng Qi, Lamei Pan, Suli Ren, Fei Chang & Rui Wang. (2020). SMTS: a swarm intelligence-inspired sensor wake-up control method for multi-target sensing in wireless sensor networks. Wireless Networks, 26 (5), 1-13.

[15] Nahid Hajizadeh, Reza Javidan, Pirooz Shamsinejad & Reza Akbari. (2020). Node deployment in wireless sensor networks using the new multi-objective Levy flight bee algorithm. IET Wireless Sensor Systems, 10 (2), 78-87.

[16] Wang Xinchen, Lyu Zengwei, Wei Zhenchun, Wang Liangliang, Lu Yang & Shi Lei. (2022). Multi-objective path planning algorithm for mobile charger in wireless rechargeable sensor networks. Wireless Networks, 29 (1), 267-283.

[17] Fattah Salmah, Ahmedy Ismail, Idris Mohd Yamani Idna & Gani Abdullah. (2022). Hybrid multi-objective node deployment for energy-coverage problem in mobile underwater wireless sensor networks. International Journal of Distributed Sensor Networks, 18 (9),

[18] Chen Long, Xu Yingying, Xu Fangyi, Hu Qian & Tang Zhenzhou. (2022). Balancing the trade-off between cost and reliability for wireless sensor networks: a multi-objective optimized deployment method. Applied Intelligence, 53 (8), 9148-9173.

[19] Gunjan. (2022). A Review on Multi-objective Optimization in Wireless Sensor Networks Using Nature Inspired Meta-heuristic Algorithms. Neural Processing Letters, 55 (3), 2587-2611.

[20] Mohtashami Hossein, Movaghar Ali & Teshnehlab Mohammad. (2022). Lifetime Improvement Based on Event Occurrence Patterns for Wireless Sensor Networks Using Multi-Objective Optimization. Wireless Personal Communications, 125 (4), 3333-3349.

[21] Natarajan Rajathi, Megharaj Geetha, Marchewka Adam, Divakarachari Parameshachari Bidare & Hans Manoj Raghubir. (2022). Energy and Distance Based Multi-Objective Red Fox Optimization Algorithm in Wireless Sensor Network. Sensors, 22 (10), 3761-3761.

[22] Jinwen Liu. (2022). Energy consumption region sensing in sensor networks based on multi-objective greedy localisation algorithm. International Journal of Information and Communication Technology, 21 (2), 137-153.

[23] Agoramoorthy Moorthy & Praveen Joe Irudaya Raj. (2021). Hybrid cuckoo–red deer algorithm for multiobjective localization strategy in wireless sensor network. International Journal of Communication Systems, 35 (4),

[24] Zhenfang Teng, Ledan Qian & Jianfei Huang. (2021). Multi-target localization algorithm for wireless sensor network. Peer-to-Peer Networking and Applications, 14 (6), 1-8.

[25] Rajani Kumari, Ruchi Kaushik & Vijander Singh. (2021). Secure Multi-objective Hybrid Routing Protocol For Wireless Sensor Network. Recent Patents on Engineering, 15 (5),

[26] Marios Krestenitis, Konstantinos Ioannidis, Stefanos Vrochidis & Ioannis Kompatsiaris. (2025). Visual to near-infrared image translation for precision agriculture operations using

GANs and aerial images. Computers and Electronics in Agriculture, 237 (PC), 110720-110720.

[27] Hao Chang, Yitian Mao, Yaohong Wang, Yingxue Lv, Dekui Yuan, Ziyu Song & Jiayi He. (2025). FFT-CNN-based target recognition for a cantilevered seal whisker model. Ocean Engineering, 339 (P1), 122076-122076.

[28] Xiaoyan Chen, Rui Huang, Yu Zhang & Qiao Zhang. (2025). DSG-SLAM: a visual SLAM for removing dynamic features and dense mapping in dynamic environments. Engineering Research Express, 7 (3), 035214-035214.

[29] Arya Paul, Anju S Pillai & Krishna Priya R. (2025). Load and congestion aware routing protocol for heterogeneous traffic loaded IoT networks. Engineering Research Express, 7 (3), 035215-035215.

[30] Wang Liang. (2025). Energy optimization in intelligent sensor networks: application of particle swarm optimization algorithm in the deployment of electronic information sensing nodes. Energy Informatics, 8 (1), 95-95.

[31] Yinghua Tong, Lianhai Lin, Liqin Tian, Zhigang Wang, Wenxing Wu & Junyi Wu. (2025). Coverage optimization and node minimization in WSNs: an enhanced hybrid PSO approach with spatial position encoding. Scientific Reports, 15 (1), 25332-25332.

[32] F. N. Gatwaza, L. Seddiki, S. Amari & H. Akdag. (2025). Distributed fault-tolerant control approach for discrete event systems using timed automata with guards: application to an electric power network. International Journal of Dynamics and Control, 13 (7), 275-275.

[33] Yao Lu. (2025). A multimodal deep reinforcement learning approach for IoT-driven adaptive scheduling and robustness optimization in global logistics networks.. Scientific reports, 15 (1), 25195.

[34] Xiaojing Zhou, Wei Wang & Yanzhong Hu. (2025). 3D ergonomics parameter measurement using video-based deep learning. Measurement, 256 (PC), 118034-118034.

[35] Javad Mozaffari, Mohammad Abdollahi Azgomi, Halimeh Madadi & Mohammad Reza Ebrahimi Dishabi. (2025). Energy and temperature-aware routing approach for congestion control in wireless body area networks. The Journal of Supercomputing, 81 (10), 1139-1139.

[36] Shuli Hu, Shuang Zhou, Dian Ling, Jiaqi Li, Ruizhi Li, Yupeng Zhou & Minghao Yin. (2025). A Multi-start Algorithm with Iterated Decremental Local Search for Minimum

Capacitated Dominating Set Problem in Large Graphs. Memetic Computing, 17 (3), 36-36.